Reentrant spin-glass-like behavior as a consequence of constrained dynamics of magnetic clusters: A case study of $Fe_{1.4}Ru_{1.6}Si$

A. K. Grover, R. G. Pillay, S. N. Mishra, D. Rambabu, and P. N. Tandon
Tata Institute of Fundamental Research, Homi Bhabha Road, Bombay-400005, India
(Received 8 December 1986; revised manuscript received 26 October 1987)

The identification of two distinct transitions in random magnetic systems as predicted by the Gabay-Toulouse model has received considerable support from ^{57}Fe Mössbauer data in Fe-based reentrant spin-glass systems. Alternatively, it has been argued that the apparent multiple-transition behavior of reentrant spin-glass alloys is a consequence of the dynamics of interacting magnetic clusters. In this picture no well-defined phase changes are expected. We present here the results of bulk-magnetic-response and ^{57}Fe-Mössbauer studies in a new random magnetic system, $Fe_{1.4}Ru_{1.6}Si$, which shows several features akin to reentrant spin glasses. The data in this system cannot be reconciled in terms of two transitions corresponding to the freezing-in of transverse and longitudinal components of the magnetic moment. Instead, our data suggest that the slowing down of spin dynamics is a continuous process, and the features that identify the reentrant spin-glass phase arise from the dynamics of mutually constrained magnetic clusters.

I. INTRODUCTION

The term reentrant spin glass (RSG) connotes the establishment of spin-glass order at a temperature below the onset of long-range magnetic order. The labeling of such a phase over a limited concentration range is a common feature of phase diagrams of all kinds of random magnetic systems, be they metallic, insulating, or amorphous. During the last few years, several groups[1–10] using Mössbauer spectroscopy have investigated $Au_{1-x}Fe_x$ and other Fe-based RSG systems and have sought to provide microscopic evidence in favor of a class of infinite-range models of spin glasses,[11–14] which sketch out a definite scenario illustrating how the transformation from paramagnetism to the RSG state via long-range ferromagnetism can come about. In particular for Heisenberg spins, Gabay and Toulouse[13] predict the existence of three transitions at T_C, T_{GT} and T_{AT}. T_C marks the onset of freezing ("ferromagnetic transition") of the longitudinal component of magnetic moments m_z^i. At T_{GT}, the transverse components m_x^i and m_y^i freeze randomly ("canting transition") such that the modulus of the total moment $|m_T^i|$ shows an anomalous increase. Finally, at T_{AT} strong irreversibility sets in with no further change in the thermal evolution of $|m_T^i|$. It is observed that in $Au_{1-x}Fe_x$ ($x=0.168$ and 0.19)[1,2,5,6] and in some other Fe-based RSG systems,[3,4,7–10] the hyperfine field averaged over all Fe nuclei H(Fe) shows an additional increase and an apparent break in slope at a temperature T_M much below the corresponding ferromagnetic ordering temperature T_C. It is also found that the magnetic moments giving rise to the hyperfine field get easily aligned in an external field between T_C and T_M and the degree of polarizability decreases below T_M. On this basis T_M has been identified with T_{GT} and from the magnetic hysteresis data in $Au_{0.81}Fe_{0.19}$ (Ref. 5), it is argued that T_{AT} may be identified as the temperature below which the coercive field shows a rapid build up.

However, such an apparently convincing line of interpretation, in particular, in the case of the $Au_{1-x}Fe_x$ system,[6,15–17] has been questioned by several groups.[18–20] A major criticism of Voilet and Borg[18] is that all the Fe nuclei do not experience similar hyperfine fields over the entire temperature range. In $Au_{1-x}Fe_x$ ($0.10 \le x \le 0.35$) (Ref. 18) alloys an analysis of Mössbauer data shows a bimodal magnetic hyperfine field distribution $P(H)$ even at the lowest temperature. Therefore, the observed $\langle H(\text{Fe})\rangle$ behavior in $Au_{1-x}Fe_x$ may be a consequence of different constituents of the distribution $P(H)$ having different temperature dependences. On the other hand, Beck[19] points out that no long-range ferromagnetism sets in at any temperature among the $Au_{1-x}Fe_x$ alloys showing the RSG behavior and that the Gabay-Toulouse model is inadequate to explain consistently the in-field and zero-field Mössbauer data in $Au_{1-x}Fe_x$ ($x=0.168$). In addition, in the RSG $Au_{0.82}Fe_{0.18}$ specimen[19] he finds that the metastability and nonequilibrium character persist over the entire temperature range across the regions of both spin glass and ferromagnetic order. In his view, the presence of magnetic short-range order and the dynamic relaxation between these clusters result in an apparent double-transition behavior. However, it has been asserted[6,15–17] that, at least in metallic[17] RSG alloys no dynamic relaxation effects are visible.

We present in this paper the results of bulk magnetic response and ^{57}Fe Mössbauer hyperfine field studies on $Fe_{1.4}Ru_{1.6}Si$. The bulk magnetization data in this system mimic many of the features of reentrant spin-glass alloys. The temperature variation of Mössbauer hyperfine field data is consistent with the interacting clusters picture of random magnetic systems. Our data suggest that the slowing down of the spin dynamics is a continuous process, and there is no identifiable phase transition at any

temperature. The results indicate that the apparent multiple-transition behavior possibly arises from short-range magnetic correlations and the constrained relaxation between dynamically interacting clusters of different sizes.

II. EXPERIMENT

The system $Fe_{1.4}Ru_{1.6}Si$

The magnetic phase diagram of the series $Fe_{3-x}Ru_xSi$ ($0 \leq x \leq 2$) has been recently established by us.[21] The end members of this series are ferromagnetic and antiferromagnetic, and for $1.5 \leq x \leq 1.7$ the alloys exhibit magnetic double-transition behavior in their ac susceptibility data. Taking $Au_{1-x}Fe_x$ as an example, it has been shown[22] that a magnetic phase diagram of the above kind can be mapped out either by varying the concentration of the magnetic atoms or by varying the degree of magnetic short-range order by giving different heat treatments to a single concentration lying in the double transition region. Following this method, we have selected the composition $Fe_{1.4}Ru_{1.6}Si$ and subjected the alloy to three different heat treatments.

The three specimens investigated are (A) as-cast ingot prepared in an arc furnace, (B) a part of this as-cast ingot annealed at 1220 K for seven days followed by quenching in water, and (C) another part of the same ingot annealed at 1220 K for seven days and furnace cooled to room temperature. All three specimens, A, B, and C are confirmed to have the cubic $L2_1$ Heusler structure. In an atomically well-ordered alloy at the stoichiometry $Fe_{1.4}Ru_{1.6}Si$, all the Ru and Si atoms would occupy (A,C) and D sites, respectively, and the Fe atoms would be distributed on all the B and the remaining (A,C) sites.[23] The three specimens essentially differ in the degree of atomic order between Fe and Si on B and D sites. The relative intensities of the x-ray reflections from the $L2_1$ superstructure indicate that the specimen B is the closest to the expected state of perfect atomic site order at this composition and is followed by the specimens C and A, respectively.[24] A simple probabilistic calculation[24] for the $L2_1$ Heusler structure reveals that the Fe concentration at the composition $Fe_{1.4}Ru_{1.6}Si$ is well above the percolation threshold required to form an infinitely linked network of Fe-Fe near neighbors. An increase in the B-D (Fe-Si) site disorder results in a decrease of the weight of the Fe atoms in this infinite cluster. Thus the specimen B, which has the least B-D site disorder among the three specimens, has the highest fraction of Fe atoms correlated into the big (infinite) cluster, while the specimen A has the highest fraction of Fe atoms in the small (finite) clusters.

The bulk-magnetic measurements made on the system under study include the low field ac-susceptibility ($\sim$0.1 Oe at 320 Hz) data (Fig. 1), the data of static magnetization versus field (M-H) up to 80 kOe at a few selected temperatures in the range 1.6–300 K, zero field cooled (ZFC) and field cooled (FC) magnetization in low fields, the thermal variation of remanence (trapped after exposing the specimen to a field of 80 kOe at 4.2 K) and the complete hysteresis loops (in specimen A only) at 4.2 and 1.6 K. The static magnetization data were obtained using an Oxford Instruments Faraday susceptometer having superconducting coils for uniform and gradient fields. The low-field ZFC and FC magnetization runs were taken after a few minutes waiting period at each setting of the temperature and field value. Figures 2–6 depict most of the static magnetization data in the three specimens.

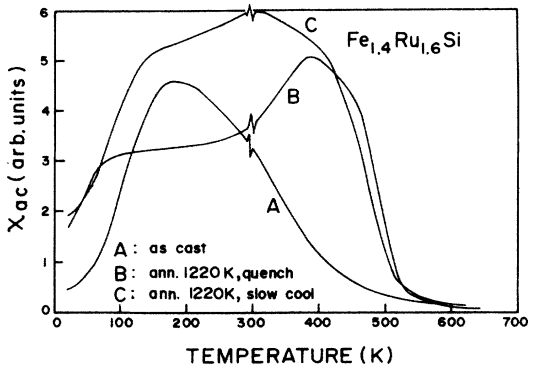

FIG. 1. ac susceptibility in the three specimens at the composition $Fe_{1.4}Ru_{1.6}Si$. A, as-cast, B, a part of the as-cast ingot annealed at 1220 K for seven days followed by quenching in water, and C, a part of the as-cast ingot annealed at 1220 K for seven days and furnace cooled to room temperature.

The ^{57}Fe Mössbauer absorption spectra with respect to $^{57}Co(Rh)$ source were recorded from 14 to 600 K in all the three specimens of $Fe_{1.4}Ru_{1.6}Si$ in a transmission geometry. Figures 7–9 display the ^{57}Fe Mössbauer spectra recorded at different temperatures along with the field distribution profiles $P(H)$ obtained using Window's method.[25] Figure 10 shows the temperature variation of the estimated average hyperfine fields in the three speci-

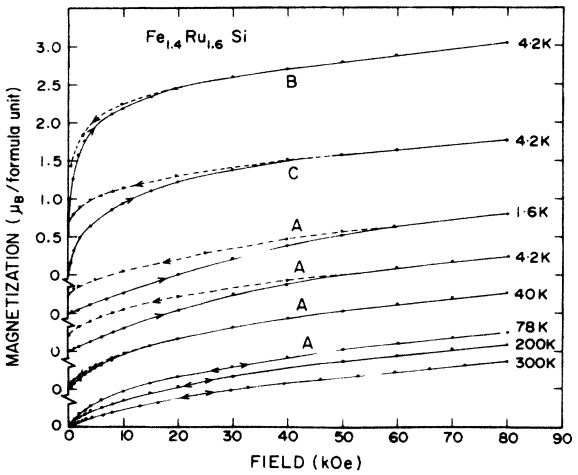

FIG. 2. Magnetization vs field data up to 80-kOe field at different temperatures in the specimens A, B, and C at composition $Fe_{1.4}Ru_{1.6}Si$. Each of the curves was obtained by cooling the specimen first to a given temperature in zero magnetic field.

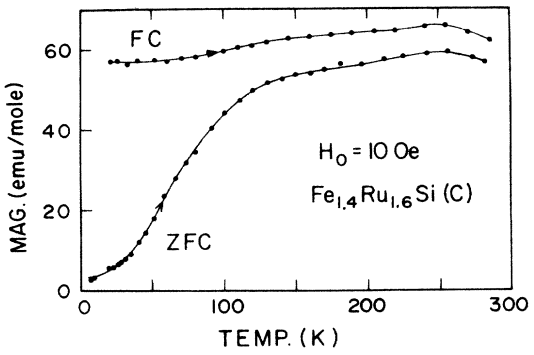

FIG. 3. Zero field cooled (ZFC) and field cooled (FC) magnetization measured in a field of 10 Oe from 4.2 to 300 K in specimen C at composition $Fe_{1.4}Ru_{1.6}Si$. FC magnetization values were recorded after having cooled the specimen to 4.2 K in a field of 10 Oe. The arrows indicate the direction in which the temperature is varied.

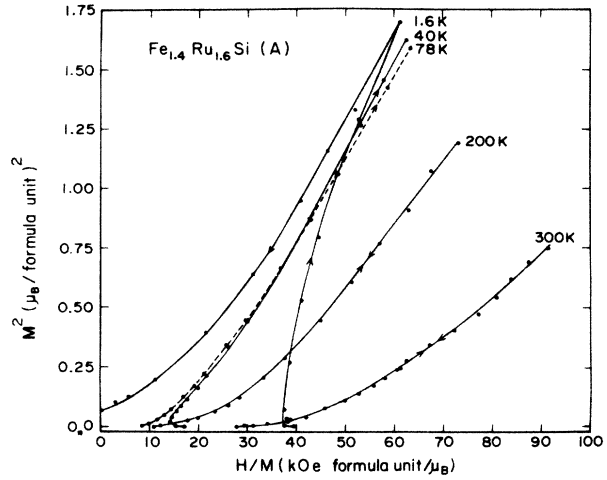

FIG. 5. Arrot plots M^2 vs H/M at different temperatures in specimen A at stoichiometry $Fe_{1.4}Ru_{1.6}Si$. The direction of field variation is indicated by arrows. At 40 and 1.6 K, M^2 vs H/M have two branches corresponding to field-up (virgin ZFC state) and field-down cycles.

mens. There is a broadening of the Mössbauer line in the paramagnetic region due to variations in the *nn* configurations and disorder in the alloys leading to possible (apparent) quadrupolar effect. We have ignored the presence of the quadrupolar effects at the Fe nuclei in fitting the Mössbauer spectra. This will, to a small extent, affect our estimates of the average hyperfine field values when they are in the range of 50 kOe. However, such an uncertainty is not expected to qualitatively alter the shape of curves of temperature variation of the average hyperfine field values. The mean value of the isomer shift and the relative absorption area $A(T)/A(300\ \mathrm{K})$ as a function of temperature are shown in Figs. 11 and 12, respectively. The mean isomer shift values have been obtained from the fitted Mössbauer spectra neglecting quadrupole effects in the fitting procedure as mentioned above. The values for the relative absorption area are estimated from the experimental spectra taking linear fits to the background from the high-velocity part of the spectra which was completely flat. Corrections due to finite-target-thickness effects were not taken into account. The signal-to-noise ratio was constantly monitored throughout the experiment to check the possible drifts in the signal level. In specimens A and B the Mössbauer spectra were also recorded at 300 K in a transverse field of 5 kOe and are shown in Figs. 13 and 14, respectively. These figures offer a comparison between the spectra recorded in zero field and applied field along with their fitted $P(H)$ distribution curves.

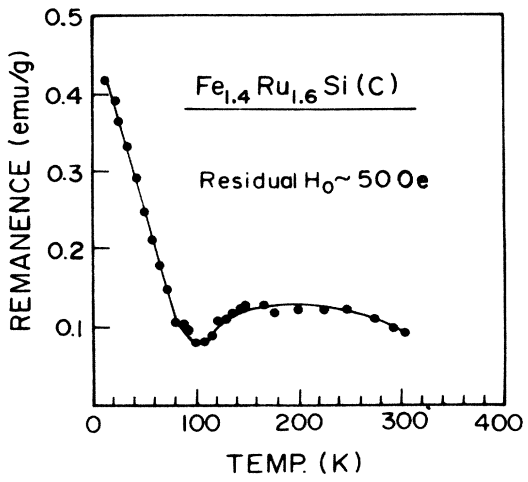

FIG. 4. Temperature variation of remanence from 4.2 to 300 K in specimen C at stoichiometry $Fe_{1.4}Ru_{1.6}Si$. The remanence data were recorded in the minimal usable field of $\lesssim 50$ Oe of the superconducting field and gradient coils. The remanence at 4.2 K was trapped after exposing the specimen to a field of 80 kOe.

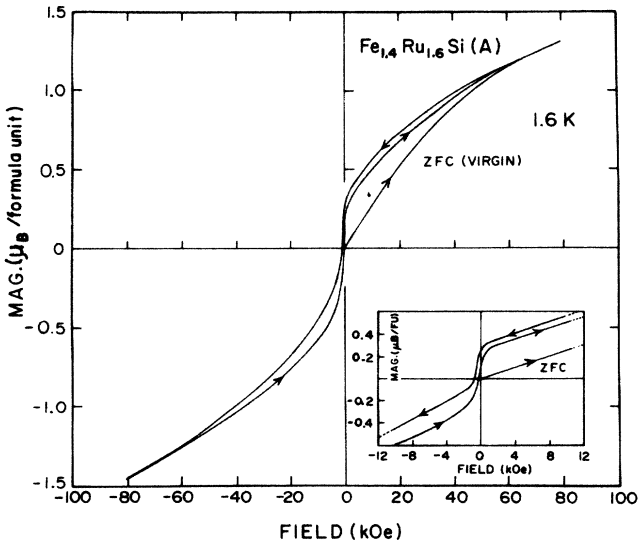

FIG. 6. Complete hysteresis loop in ±80-kOe field at 1.6 K in specimen A at composition $Fe_{1.4}Ru_{1.6}Si$. The inset shows the blow up of the data near the origin.

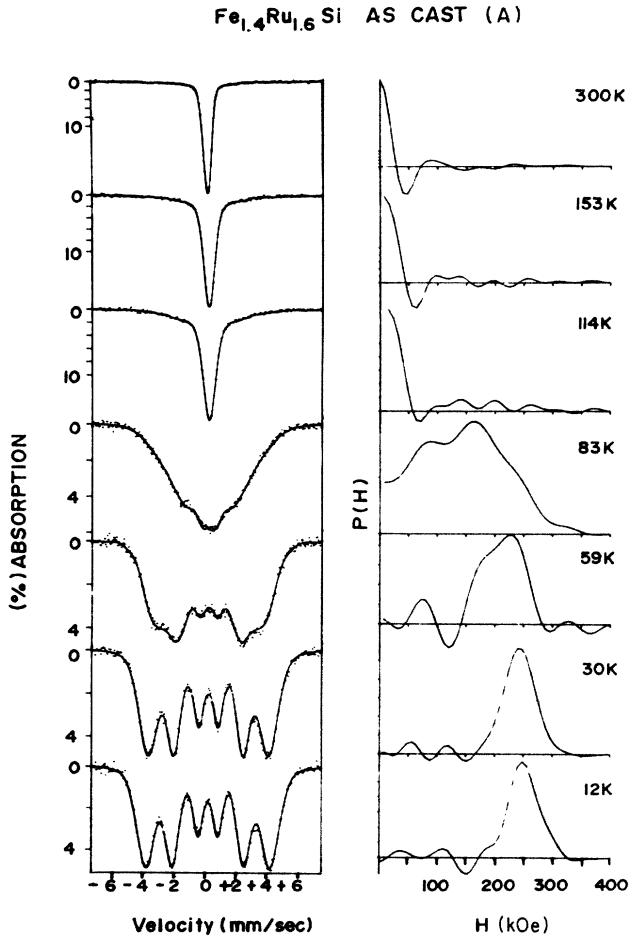

FIG. 7. ^{57}Fe Mössbauer spectra and the fitted hyperfine field distributions at different temperatures in specimen A at composition $Fe_{1.4}Ru_{1.6}Si$.

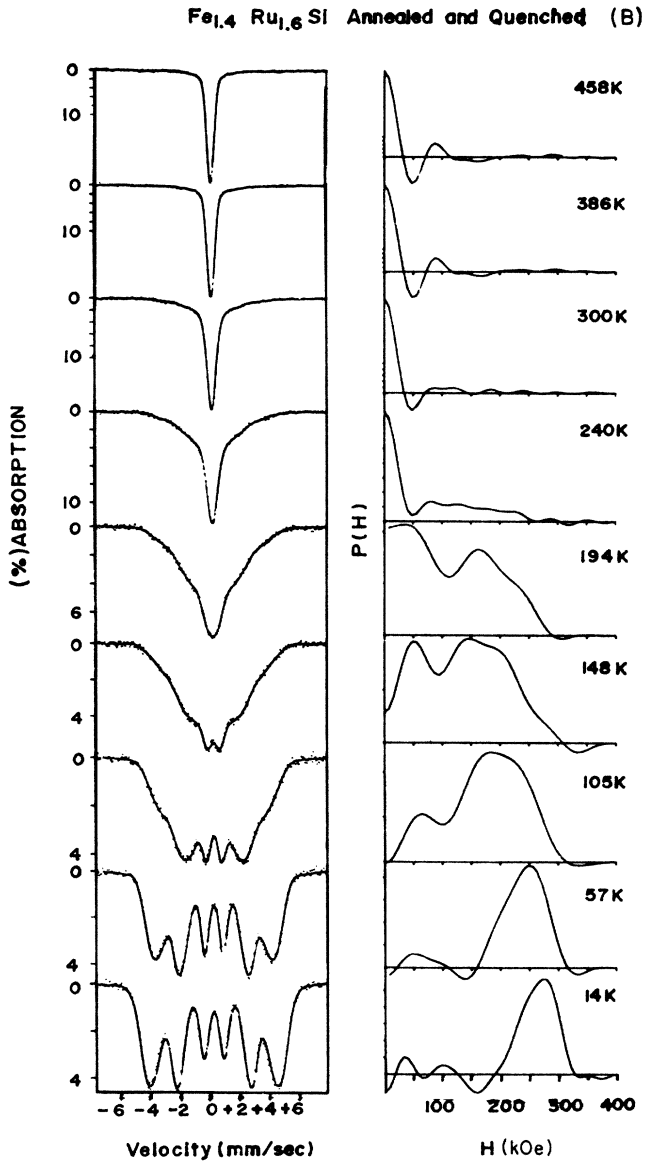

FIG. 8. ^{57}Fe Mössbauer spectra and the fitted hyperfine field distributions at different temperatures in specimen B at composition $Fe_{1.4}Ru_{1.6}Si$.

III. RESULTS AND ANALYSIS

A. Bulk magnetic behavior

The ac susceptibility measurements were made on arbitrarily shaped specimens and the data of Fig. 1 have not been corrected for shape-dependent demagnetization effects. The ac-susceptibility curves (in arbitrary units) (Fig. 1) for specimens B and C show two apparent transitions: an upturn near 500 K followed by a down turn at lower temperature, whereas for specimen A only a composite and broad bell shaped maximum is visible. In view of the arbitrariness in χ_{ac} units and in the absence of demagnetization corrections we tentatively identify the two apparent transitions in χ_{ac} data of Fig. 1 with ferromagneticlike response and the spin-glass order as in reentrant spin-glass systems. Magnetization versus field data of Fig. 2 show that the specimens A, B, and C widely differ in the degree of polarizability and the magnetization values attained in a field of 80 kOe at 4.2 K. The specimen B, which shows least-hysteretic behavior, is the easiest to polarize and acquires the largest magnetization value of 3.0 μ_B formula unit (which is equivalent to 2.2 μ_B/Fe atom) in 80 kOe at 4.2 K. It is followed by specimens C and A with the magnetization values of 1.25 μ_B/(Fe atom) and 0.9 μ_B/(Fe atom), respectively, at 4.2 K. The ac-susceptibility values in Fig. 1 are not presented in absolute units; however, it is apparent that at room temperature ($\sim$300 K) none of the three specimens are in the conventionally understood paramagnetic state. The curvature of the M vs H plot at 300 K in specimen A (Fig. 2), which has the least-magnetization value at 4.2 K, confirms that even this specimen is not in the paramagnetic state at room temperature.

In all the three specimens, the degree of polarizability in low fields ($H < 10$ kOe) decreases and that of irreversibility increases on cooling below 80 K. These facts are well brought out by the M vs H curves at various temper-

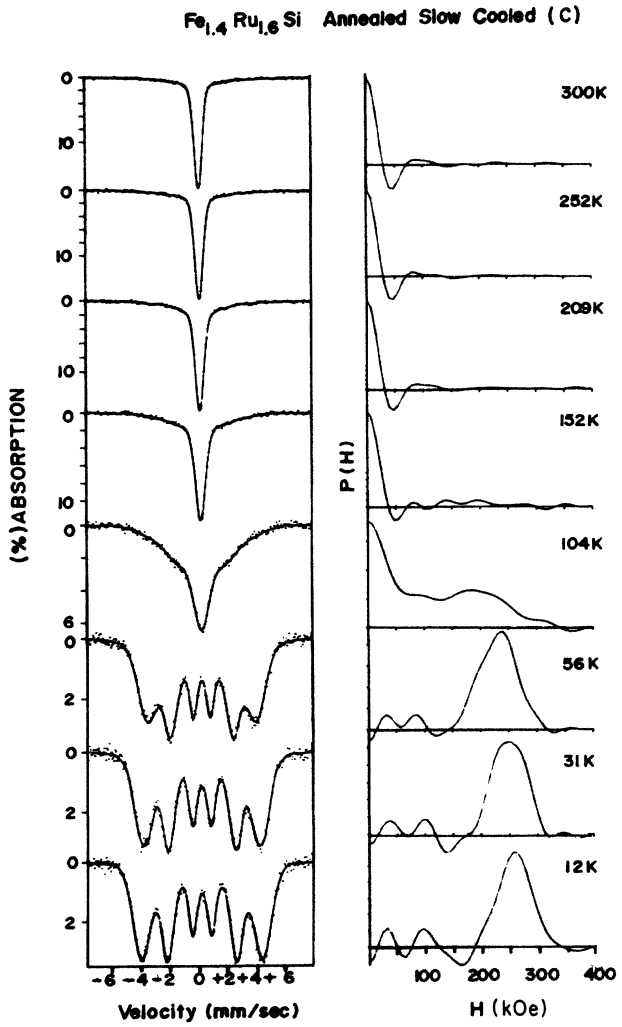

FIG. 9. ^{57}Fe Mössbauer spectra and the fitted hyperfine field distributions at different temperatures in specimen C at composition $Fe_{1.4}Ru_{1.6}Si$.

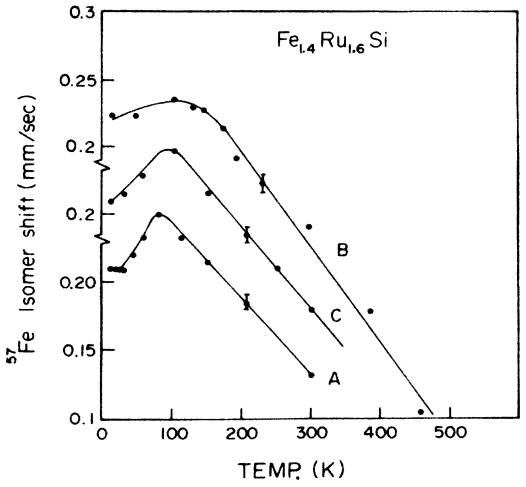

FIG. 11. Temperature variation of mean isomer shift at ^{57}Fe with respect to natural Fe in specimens, A, B, and C at stoichiometry $Fe_{1.4}Ru_{1.6}Si$.

atures. Figure 2 shows the data only in specimen A. The sample shows negligible hysteresis in the M vs H curves at 78 K. However, the hysteresis loop (data shown in one quadrant in Fig. 2) starts to open up rapidly below $\sim$40 K, which is significantly below the temperature region of downturn in ac susceptibility.

Figure 3 shows the difference between zero field cooled and field cooled ($H=10$ Oe) magnetization in the specimen C. The ZFC and FC magnetization values were recorded during the warmup cycle from 4.2 to 300 K. The data above 300 K could not be taken because of the limitations in our experimental set up. The data in the other two samples were similar to that in specimen C. It is seen (Fig. 3) that the ZFC and FC curves do not overlap up to 300 K. This may be taken as additional evidence that the samples are not in the paramagnetic state at 300 K. We expect the difference between ZFC and FC

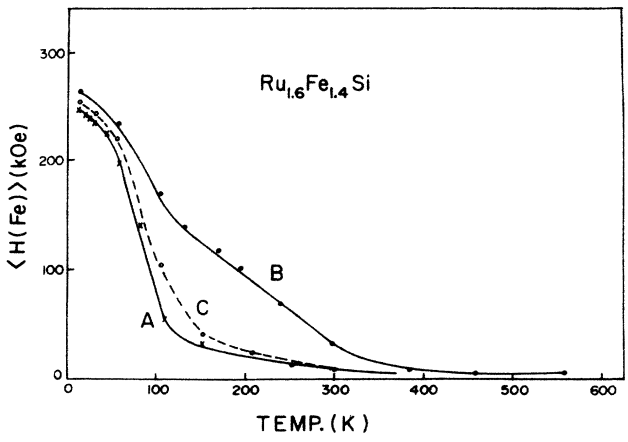

FIG. 10. Temperature variation of average hyperfine field values computed from the fitted field distributions in the three specimens at composition $Fe_{1.4}Ru_{1.6}Si$.

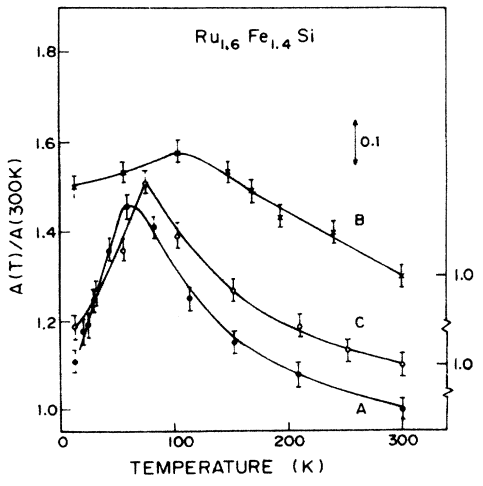

FIG. 12. Temperature variation of relative area $A(T)/A(300\text{ K})$ under the ^{57}Fe Mössbauer absorption curves in the three specimens at composition $Fe_{1.4}Ru_{1.6}Si$.

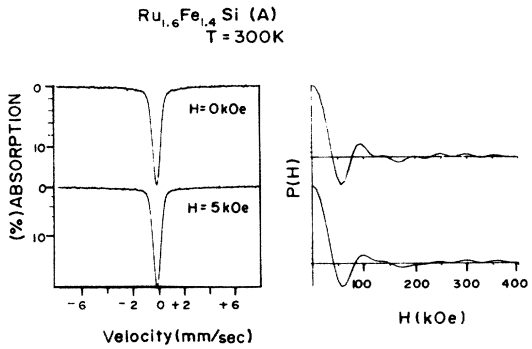

FIG. 13. ^{57}Fe Mössbauer spectra at 300 K in 0- and 5-kOe transverse-field values in specimen A at composition $Fe_{1.4}Ru_{1.6}Si$.

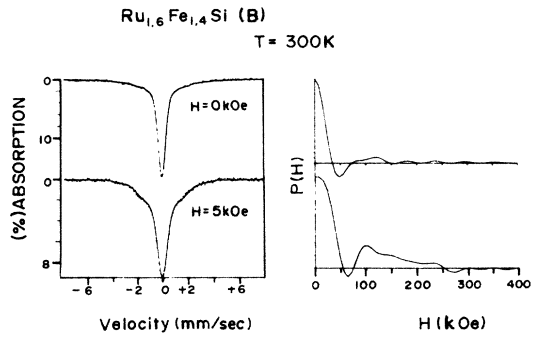

FIG. 14. ^{57}Fe Mössbauer spectra at 300 K in 0- and 5-kOe transverse-field values in specimen B at composition $Fe_{1.4}Ru_{1.6}Si$.

magnetization to persist up to the paramagnetic region in all the three specimens in consonance with Beck's[19] data in $Au_{0.82}Fe_{0.18}$ alloy. Figure 4 displays the thermal decay of remanence in specimen C from 4.2 to 300 K. This data was recorded in the minimum usable field (<50 Oe) of the superconducting field and gradient coils assembly. Most of the remanent magnetization, trapped at 4.2 K after exposing the specimen to a field of 80 kOe, decays on heating the specimen to about 100 K. The podgy hump visible in the temperature region of 100–300 K (Fig. 4) is due to unavoidable superposition of the magnetization in a field of $\lesssim 50$ Oe of the field cycled specimen.

The increase in the difference between ZFC and FC magnetization values below 100 K and the remanence data point towards some transformation in the magnetic behavior of the three specimens in the 100 K region, namely, into the strongly irreversible state. However, the fact that significant difference between FC and ZFC magnetization values is present even above the temperature region of downturn in ac susceptibility shows that the alloy system remains in a nonequilibrium state far above this region. Arrot plots confirm that there is no spontaneous magnetization, thereby implying the absence of ferromagnetism in the ZFC state of all the three specimens at any temperature. Figure 5 shows the M^2 vs H/M curves in specimen A (data in other two specimens not plotted here). For $T<78$ K, each of the M^2 vs H/M curves has two branches corresponding to field-up (virgin ZFC state) and field-down cycles. In the limit $H/M\rightarrow 0$, there is no positive intercept on the M^2 axis (hence no spontaneous magnetization) at $T\geq 78$ K. Also, below 78 K, there is no spontaneous magnetization in the virgin ZFC state of the specimen. Finite intercepts on the M^2 axis are observed on extrapolating the data recorded during the field-down cycle for $T\leq 40$ K. The virgin branches for 40 and 1.6 K cut across the 78-K curve at increasing value of H/M. This just reflects an increasing difficulty in polarizing all the moments for $T<78$ K. The 80-kOe magnetization value remains nearly the same as T decreases from 78 to 1.6 K. Another interesting fact evident from Fig. 5 relates to the change in character of M vs H curves in low field ($\sim 1-2$ kOe) values for $T\lesssim 40$ K. The knee in the initial portion of the M^2 versus H/M curves at 1.6 and 40 K corresponds to an initial susceptibility increase followed by a decrease as a function of the external field. This kind of transformation is seen in systems which display field-induced quasiferromagnetic behavior from a virgin antiferromagneticlike state.

Figure 6 shows the complete hysteresis loop in specimen A at 1.6 K. The main characteristics of this loop are the following. (1) The virgin (ZFC) M vs H curve lies outside the loop traced on cycling the specimen between ± 80 kOe. (2) The loop is not symmetric with respect to both the axes. Its center of gravity is shifted towards negative-field values (see the inset of Fig. 6); this is reminiscent of the well-documented behavior in several spin-glass systems.[26] It is also interesting to find that the magnetization value at $+80$ kOe is smaller than the value at -80 kOe. (3) An almost linear variation of M vs H in fields up to 10 kOe in the ZFC state (see the inset of Fig. 6) clearly indicates that the moments are randomly oriented in the virgin state. However, after cycling the specimen in ± 80 kOe, the shape of the M vs H curves appears to be made up of superposition of a randomly oriented spin-glass component and an easily polarizable ferromagnetic part. In fact, after field cycling, the observed shape of the loop is similar to that recorded at higher temperatures ($T\geq 78$ K), the only difference being that for $T\geq 78$ K there are almost no remanence and hysteresis. It is not out of place to recall here that after field cycling the shape of the hysteresis loop at 1.6 K is akin to the anomalous constricted hysteresis loops seen in many magnetic rocks.[27] The behavior in rocks has been shown[27] to be a composite response from two physically distinct magnetic components; however, in the present case the exposure to high-magnetic field causes the virgin homogeneous state to behave like superposition of two components.

B. Mössbauer results

It is very instructive to compare the bulk-magnetization data in the three specimens of $Fe_{1.4}Ru_{1.6}Si$ with their Mössbauer results. Figures 7–9 show that for $T\lesssim 30$ K, the Mössbauer spectra and the fitted hyperfine

field distributions in all three specimens look similar. The average hyperfine field values at Fe nuclei at ~ 13 K range from 250 to 270 kOe (Fig. 10) with a narrow distribution of ± 35 kOe (HWHM). This seems to imply that at the atomic moment level the three samples have similar behavior for $T \lesssim 30$ K. The magnitude of the $\langle H(\mathrm{Fe}) \rangle$ value of ~ 270 kOe in specimen B is compatible with its magnetization value of 2.2 μ_B/Fe atom at 4.2 K in 80 kOe, but in the specimens C and A the corresponding magnetization values are much lower as M vs H curves do not show inclination towards saturation up to 80-kOe field.

The comparison of the thermal evolution of $\langle H(\mathrm{Fe}) \rangle$ (Fig. 10) in the three specimens with their corresponding ac-susceptibilities (Fig. 1) reveals that even though the specimens B and C have similar ac-susceptibility response, they differ vastly in the nature of their $\langle H(\mathrm{Fe}) \rangle$ evolution. The $\langle H(\mathrm{Fe}) \rangle$ for specimen B starts to evolve around 400 K and shows an additional increase in the temperature region of the downturn in the ac-susceptibility curve (cf. Figs. 1 and 10). This is analogous to the behavior in many RSG systems described in Sec. I and is sought to be interpreted as freezing of longitudinal and transverse components of Fe moments in the Gabay-Toulouse picture.[1,2] However, such an identification cannot be sustained in the present system, which is evident from a comparison of $\langle H(\mathrm{Fe}) \rangle$ curves in specimens C and A. In specimen C, which shows a double transition in the ac-susceptibility response, the $\langle H(\mathrm{Fe}) \rangle$ value (Fig. 10) shows a very gentle rise down to ~ 150 K and only below this a rapid buildup sets in. The $\langle H(\mathrm{Fe}) \rangle$ value in specimen C at ~ 150 K (which is far below its $T_C \sim 500$ K) is less than 20% of its ultimate value at the lowest temperature. The specimen A, which does not show any reentrant like feature in ac-susceptibility behavior, has similar $\langle H(\mathrm{Fe}) \rangle$ variation as in specimen C.

If we closely examine the Mössbauer spectra and their fitted hyperfine field distributions [$P(H)$] in Figs. 8 and 9, it is evident that the difference in $\langle H(\mathrm{Fe}) \rangle$ vs T curves for specimens B and C (Fig. 10) may be a consequence of different constituents of $P(H)$ having different temperature variations. Up to about 56 K (cf. Figs. 7 to 9), the $P(H)$ in all the three specimens appear similar with a fairly narrow distribution. Above this temperature an additional lower-field bundle builds up, thus reducing the $H(\mathrm{Fe})$ in all three specimens. In the temperature range $T \gtrsim 150$ K the Mössbauer pattern collapses into a single line more rapidly in A and C (Figs. 7 and 9) as compared to that in B (Fig. 8).

The change in slope of $\langle H(\mathrm{Fe}) \rangle$ versus temperature near the 100 K region is a feature common to the three specimens of $Fe_{1.4}Ru_{1.6}Si$ (cf. Fig. 10). The thermal variation of the mean isomer shift (IS) with respect to natural Fe absorber and the relative area under the Mössbauer absorption curves $A(T)/A(300\ \mathrm{K})$ in all the three specimens are depicted in Figs. 11 and 12, respectively. There is no sound reason to expect any anomalous variation of these two quantities in the temperature region of a slowdown of Fe spin dynamics. As stated earlier the data of Figs. 11 and 12 may suffer from the artifact of the fitting procedure adopted by us in estimating these two quantities; nevertheless, it is thought provoking to find that both IS and $A(T)/A(300\ \mathrm{K})$ show downturn around the temperature region where $\langle H(\mathrm{Fe}) \rangle$ values show a rapid buildup. The downturns are somewhat less pronounced in specimen B as compared to those in C and A. It should be mentioned here that in other compositions ($0 \leq x \leq 1.35$) of the series $Fe_{3-x}Ru_xSi$, which do not exhibit any transformation in the low-temperature region in their bulk-magnetic response,[21] no such downturns are observed in the temperature dependence of IS and $A(T)/A(300\ \mathrm{K})$ values.[24,28] In these compositions, both the parameters show monotonic increase with decreasing temperature, and the observed temperature variations of IS and relative absorption area can be accounted for in terms of the second-order Doppler shift and the Debye-Waller effect, respectively.[24,28]

Figures 13 and 14 show that in both the specimens A and B the application of an external magnetic field results in an increase in the magnitude of $\langle H(\mathrm{Fe}) \rangle$ values at room temperature which is below the paramagnetic region (see χ_{ac}- and dc-magnetization data). The change is pronounced (~ 20 kOe) in sample B as compared to that (~ 5 kOe) in sample A. In the paramagnetic state, the external field of 5 kOe is expected to get reflected as an internal field of 5 kOe as seen by the Fe nucleus. Whereas, in the ferromagnetic state this should result in an increase or decrease of ≤ 5 kOe depending on the sign of the internal field experienced by the Fe nucleus. The observed increase of ~ 20 kOe at 300 K in sample B cannot be reconciled in terms of either truly paramagnetic or ferromagnetic or admixture of macroscopically distinct quasiferromagnetic and paramagnetic regions. This result is similar to the increase in the magnitude of $H(\mathrm{Fe})$ values in the RSG alloy $Au_{0.832}Fe_{0.168}$ (Ref. 4). Beck[19] pointed out that the observed increase in the latter system is opposite to the expected decrease in a normal ferromagnet. The negative sign of the hyperfine field at Fe should result in a decrease in the magnitude of $H(\mathrm{Fe})$ in an external field.

IV. DISCUSSION

The results presented in Sec. III have clearly shown that the three specimens under consideration are in a nonequilibrium state over the temperature range, encompassing the region of initial rise in ac susceptibility, down to the lowest temperature. The magnetic-hysteresis data vividly demonstrate the metastable and irreversible nature at low temperatures. There is no hard evidence for the existence of genuine ferromagneticlike phases in the zero field cooled state at any temperature below the paramagnetic region. However, on exposing the specimen to a high-magnetic field or cooling the specimen in a finite field can induce a quasiferromagnetic response in the system. Further, the data give evidence for some transformation in the magnetic behavior of the system in the temperature region of the downturn in the ac-susceptibility response. We believe that the Mössbauer data (Figs. 7–10) are providing us with the clues to understanding the mechanism of this transformation.

The observed Mössbauer patterns of Figs. 7–9 have been fitted to static hyperfine field distributions. The fitted $P(H)$ for $T_C > T > 100$ K indicate the presence of a wide distribution of field values. It is to be noted that in this temperature region the Mössbauer spectra consist of a central paramagnetic line along with unresolved wings. A closer examination of these Mössbauer spectra clearly points towards the existence of dynamic relaxation effects,[29–31] with the mean tumbling frequency of the Fe moments to be of the same order as the Larmor precession frequencies ($\sim 10^7$ s^{-1}). Such an inference finds support from the comparison of in-field and zero-field Mössbauer patterns at 300 K (Figs. 13 and 14). The increase in $\langle H(\mathrm{Fe})\rangle$ values on application of an external field disfavors the resolution of the observed Mössbauer spectra in terms of static field distributions.

The fact that the difference between ZFC and FC magnetization values persists up to the paramagnetic region implies the presence of very long relaxation times. Thus the Mössbauer and magnetization data demand the existence of a wide distribution of relaxation times of the Fe moments below the paramagnetic state. The spectral range extends from a much shorter than Mössbauer time window of $\sim 10^{-7}$ s to much longer times (at least $\sim$ few minutes). The mean weight of the distribution is seen to move towards longer times as the temperature is lowered. We believe that the differences between the three specimens of $Fe_{1.4}Ru_{1.6}Si$ in their hyperfine field behavior originate from the different spectral distribution of the tumbling frequencies and their thermal evolutions. In specimens A and C (see Figs. 7 and 9) above ~ 150 K most of the weight of Mössbauer spectra is in the central paramagnetic line. These indicate that only a fraction of Fe moments tumble slower than 10^{-7} s for $T \gtrsim 150$ K. The tumbling times of most of the Fe moments in samples A and C are seen to become slower than the Mössbauer time scale only below 150 K. Specimen B, however, differs from the other two in having a much larger fraction of Fe moments having tumbling times slower than $\sim 10^{-7}$ s, even above ~ 150 K. The shapes of Mössbauer spectra between 150 and 80 K in all specimens indicate that the dynamic relaxation effect gives way to the static hyperfine fields for all the Fe nuclei only below ~ 80 K. The interval 150 to 80 K roughly overlaps with the temperature region of the steep fall in the ac-susceptibility curves. This suggests that there exists strong coupling between the degrees of freedom corresponding to short and long relaxation times. The static hyperfine field split pattern for all the nuclei emerges only when the dynamics of the fastest degree of freedom slows down.

The broad spectrum of relaxation times can arise from magnetic clusters of various shapes and sizes. The bigger sized clusters probably[32] are easier to polarize and have longer relaxation times. The chemical short-range order in each specimen determines the magnetic cluster distribution. However, their size and morphology are expected to undergo continuous thermal evolution and temporal variation. We feel that the predominance of the small (finite) clusters dictate the behavior of specimens A and C, whereas in specimen B, a sufficient fraction of Fe atoms get correlated into big-sized clusters above ~ 150 K. The dynamic relaxation effect between Fe moments comprising the different clusters, however, prevent the appearance of well-resolved splitting in the Mössbauer spectra above ~ 150 K even in specimen B. The transformation in the magnetic behavior occurring below ~ 100 K is due to the slowing down of dynamics of the smallest clusters. It is pertinent to recall here that analogous inferences have been drawn earlier by Sarkissian[33] and more recently by Mirza and Loram[34] from their analyses, respectively, of electron spin resonance and specific heat data in $Au_{1-x}Fe_x$ alloys. In particular, Mirza and Loram[34] find that the lower temperature anomaly in specific heat involves disordering of all spins lying in both infinite- and finite-sized clusters. On the basis of their data, they argue that magnetization of the ferromagnetic infinite cluster is pinned when the network of Fe spins of lower coordination number in which it is immersed orders as a spin glass. It may appear fortuitous, but it is interesting to note that the experimental data in different reentrant spin-glass systems echo one of the essential basis of a class of theoretical models for relaxation in strongly interacting glasses due to Palmer, Stein, Abrahams, and Anderson (PSSA).[35] PSSA remark that a hierarchical scheme in which faster degrees of freedom successively constrain the slower ones seems the only natural way to generate a wide range of relaxation times in glassy systems.

V. SUMMARY AND CONCLUSIONS

The results of ac-susceptibility, dc-magnetization, and ^{57}Fe-Mössbauer studies in a new reentrant spin-glass system $Fe_{1.4}Ru_{1.6}Si$ have been described. The observed temperature variation of hyperfine field data at Fe nuclei in these alloys cannot be reconciled in terms of freezing of all the magnetic moments in homogeneous "collinear ferromagnetic" and "canted ferromagnetic" phases at different temperatures as per the mean-field approach of Gabay and Toulouse.[13] The Mössbauer data in conjunction with thermomagnetic effects confirm the existence of wide spectrum of relaxation times below the paramagnetic region, and this favors the picture of interacting magnetic clusters for this system. The slowdown of spin dynamics is a continuous process. The ac susceptibility in a given specimen is presumably the envelope of responses of these interacting magnetic clusters.[36,37] The comparison of thermal evolution of Mössbauer spectra in the different specimens, containing the same concentration of magnetic ions but with different distributions in cluster sizes, has shown that the slowly moving big clusters are coupled to the faster moving small clusters. It is the ultimate slowing down of the dynamics of the small clusters that constrains the overall spin dynamics and give rise to the appearance of the so-called reentrant or simply the spin-glass state.

If in the present investigations evidence for the chemical homogeneity of the specimens and the existence of nonequilibrium and dynamical relaxation effects over a wide temperature range are completely disregarded, the

observed Mössbauer behavior in the three specimens of $Fe_{1.4}Ru_{1.6}Si$ A, C, and B may be understood as cluster spin glasses with increasing amount of macroscopically distinct ferromagnetic lumps in them. In such a circumstance, the resolution of the spectra in terms of static hyperfine field distribution can be considered adequate. However, our[38,39] recent Mössbauer observations in other widely investigated systems by several groups,[40] namely, $(Pt_{1-x}Pd_x)_3$ Fe ($x \sim 0.5$) and $Pt_3(Fe_{1-x}Mn_x)$ ($x \sim 0.6$), lend more credit to the $Fe_{1.4}Ru_{1.6}Si$ system described in terms of interacting clusters. The phase diagrams of both these ternary series[40] indicate the occurrence of multiple-magnetic transitions for concentrations in which RSG phase is believed to be present at the lowest temperature. It has been found[38,39] that the ^{57}Fe-Mössbauer spectra in these alloys do not take cognizance of the higher-temperature transitions visible in the ac-susceptibility data. Static hyperfine splittings become visible only on approaching the lowest transition identifying the reentrant spin-glass phase. The temperature variation of average hyperfine field values at Fe nuclei show behavior[38] somewhat similar to that reported in $Au_{0.832}Fe_{0.168}$ alloy showing double transition.[2] We believe that there broadly exist three temperature regimes in reentrant spin-glass systems investigated by us. They are the high-temperature paramagnetic region, the low-temperature spin-glass state, and the intermediate region. The magnetic behavior in the intermediate region is dominated by the presence of slowly moving big clusters which are capable of giving quasiferromagnetic response in an external magnetic field. In Beck's view[19] the presence of quasirandom anisotropy, which largely determines the local orientation of the cluster moments at low temperatures in the zero field cooled state, identifies the low-temperature spin-glass region. Such an anisotropy can arise from geometrical shapes of clusters. As the temperature is raised the thermal activation can free the cluster moments from the constraints of local anisotropy. It is intriguing to find the signature of locking of Fe moments into random orientation in the temperature dependences of ^{57}Fe isomer shift and recoil-free fraction in $Fe_{1.4}Ru_{1.6}Si$ alloys (see Figs. 11 and 12). These suggest an interesting possibility of accompanying changes in the electron-magnon and electron-phonon couplings due to a local magnetostrictive effect from spin-glass-type ordering. Anomalous changes in these couplings have been reported to occur across magnetic ordering in some Heusler alloys.[41]

Finally it is fruitful to compare the Mössbauer behavior in reentrant spin-glass alloys investigated by us with the dilute magnetic alloys. In some dilute magnetic alloy systems,[42,43] the recent detailed investigations have revealed the presence of dynamic relaxation effects up to the temperature limit of 1.5 T_{SG}. Thus even in the simple spin-glass system the three temperature regimes can be identified. Ogielski[44] and Campbell[45–47] have attempted to explain the existence of three different regions for relaxation in spin glasses on the basis of their computational work for a finite number of Ising spins. In the physical picture conceived by Campbell, the magnetic system executes random walks on a closed surface in phase space. At high temperature all eigenstates are mutually accessible (paramagnet). As the temperature is lowered the allowed set of states thin out to a ramified network, and then at percolation threshold they fragment into discontinuous subnetworks. The spin-glass transition is identified with the percolation threshold in eigenstate space. In the spin-glass state the system will become nonpercolating and hence nonergodic and highly irreversible. The intermediate state in which the system has access over a ramified lattice of phase points show a stretched exponential relaxation. Thus on the laboratory timescale a weak irreversibility and metastability would be observed in the intermediate state. We believe that in concentrated magnetic alloys (above the percolation threshold for nearest-neighbor ferromagnetic links), this intermediate region lying in between the paramagnetic and spin-glass states gets extended over a wider temperature range as compared to that in dilute spin-glass systems. Thus the experimental results presented in this paper seem to imply that the inferences arrived at by Ogielski and Campbell are applicable to real systems.

ACKNOWLEDGMENTS

We would like to thank Dr. I. A. Campbell for helpful discussions. It is a pleasure to acknowledge useful conversations with Dr. V. C. Rakhecha, Dr. A. P. Murani, and Professor D. E. Maclaughlin. We also thank Professor C. Radhakrishnamurty, Professor H. G. Devare, and Professor R. Vijayaraghavan for their continued interest in this work.

[1] J. Lauer and W. Keune, Phys. Rev. Lett. **48**, 1850 (1982).

[2] F. Varret, A. Hamzic, and I. A. Campbell, Phys. Rev. B **26**, 5289 (1982).

[3] V. Manns, R. A. Brand, W. Keune, and R. Marx, Solid State Commun. **48**, 811 (1983).

[4] R. A. Brand, V. Manns, and W. Keune, in *Heidelberg Colloquium on Spin Glasses,* Vol. 192 of *Lecture Notes in Physics,* edited by J. L. van Hemmen and I. Morgenstern (Springer, Berlin, 1983), p. 79, and references therein.

[5] I. A. Campbell, S. Senoussi, F. Varret, J. Teillet, and A. Hamzic, Phys. Rev. Lett. **50**, 1615 (1983).

[6] R. A. Brand, J. Lauer, and W. Keune, Phys. Rev. B **31**, 1630 (1985); M. M. Abd-Elmeguid, H. Micklitz, R. A. Brand, and W. Keune, *ibid.* **33**, 7833 (1986).

[7] Y. Takeda, S. Morimoto, A. Ito, T. Sato, and Y. Miyako, J. Phys. Soc. Jpn. **54**, 2000 (1985).

[8] I. Mirebeau, G. Jehanno, I. A. Campbell, F. Hippert, B. Hennion, and M. Hennion, J. Magn. Magn. Mater. **54-57**, 99 (1986).

[9] R. A. Brand, H. Georges-Gilbert, J. Hubsch, and J. A. Heller,

J. Phys. F **15**, 1987 (1986).
[10]P. L. Paulose, V. Nagarajan, R. Nagarajan, and R. Vijayaraghavan, Solid State Commun. **61**, 151 (1987).
[11]D. Sherrington and S. Kirkpatrik, Phys. Rev. Lett. **35**, 1792 (1975); Phys. Rev. B **17**, 4384 (1978).
[12]J. R. L. de Almeida and D. J. Thouless, J. Phys. A **11**, 983 (1978).
[13]M. Gabay and G. Toulouse, Phys. Rev. Lett. **47**, 201 (1981).
[14]D. M. Cragg, D. Sherrington, and M. Gabay, Phys. Rev. Lett. **49**, 158 (1982).
[15]P. Monod and I. A. Campbell, Phys. Rev. Lett. **52**, 2096 (1984).
[16]R. A. Brand and W. Keune, Phys. Rev. Lett. **52**, 2097 (1984).
[17]I. A. Campbell, Hyperfine Int. **27**, 15 (1986).
[18]C. E. Violet and R. J. Borg, Phys. Rev. Lett. **51**, 1073 (1983); **52**, 2098 (1984).
[19]P. A. Beck, Phys. Rev. B **32**, 7255 (1985), and his papers listed therein.
[20]G. Apeppli, S. M. Shapiro, H. Maletta, R. J. Birgeneau, and H. S. Chen, J. App. Phys. **55**, 1628 (1984).
[21]D. Rambabu, S. N. Mishra, A. K. Grover, R. G. Pillay, P. N. Tandon, H. G. Devare, and R. Vijayaraghavan, in *Proceedings of the Second Asia Pacific Physics Conference,* Bangalore, India, 1986, edited by S. Chandrashekar (World Scientific, Singapore, 1987), p. 855.
[22]S. Crane and H. Claus, Phys. Rev. Lett. **46**, 1693 (1981); G. Griffith and H. Claus, J. Magn. Magn. Mater. **54-57**, 151 (1986), and references therein.
[23]S. N. Mishra, D. Rambabu, A. K. Grover, R. G. Pillay, P. N. Tandon, H. G. Devare, and R. Vijayaraghavan, Solid State Commun. **53**, 321 (1985); J. App. Phys. **57**, 3258 (1985).
[24]S. N. Mishra, Ph.D. thesis, University of Bombay, India, 1986.
[25]B. Window, J. Phys. E **4**, 401 (1971).
[26]J. J. Prejean, M. J. Joliclerc, and P. Monod, J. Phys. (Paris) **41**, 427 (1980); R. W. Knitter, J. S. Kouvel, and H. Claus, J. Magn. Magn. Mater. **5**, 356 (1977).
[27]C. Radhakrishnamurthy and P. W. Sahasrabudhe, Curr. Sci. **11**, 338 (1965).
[28]S. N. Mishra, D. Rambabu, A. K. Grover, R. G. Pillay, and P. N. Tandon (unpublished).
[29]H. H. Wickman, Mössbauer *Effect Methodology* (1966), Vol. V, p. 39.
[30]H. Schwegler, Fortschr. Phys. **20**, 251 (1972).
[31]K. Krop, J. Korecki, J. Zukrowski, and W. Karas, Int. J. Magnetism **6**, 19 (1974).
[32]A. K. Grover, L. C. Gupta, R. Vijayaraghavan, M. Matsumura, N. Nakano, and K. Asayama, Solid State Commun. **30**, 457 (1979); A. K. Grover, S. K. Malik, C. Radhakrishnamurthy, and R. Vijayaraghavan, *ibid.* **32**, 1323 (1979).
[33]B. V. B. Sarkissian, Philos. Mag. **39**, 413 (1979).
[34]K. A. Mirza and J. W. Loram, J. Phys. F **15**, 439 (1985).
[35]R. G. Palmer, D. L. Stein, E. Abrahams, and P. W. Anderson, Phys. Rev. Lett. **53**, 958 (1984).
[36]E. P. Wohlfarth, Phys. Lett. **70A**, 489 (1979).
[37]S. Shtrikman and E. P. Wohlfarth, Phys. Lett. **85A**, 467 (1981).
[38]A. K. Grover, R. G. Pillay, S. N. Mishra, D. Rambabu, and P. N. Tandon, Hyperfine Int. **34**, 523 (1987).
[39]A. K. Grover, L. C. Tribedi, R. Nagarajan, J. Y. Yakhimi, and L. C. Gupta (unpublished).
[40]W. Stamm and F. Wassermann, J. Magn. Magn. Mat. **54-57**, 161 (1986).
[41]K. K. Wang, P. Boolchand, J. Scanlon, and P. Jena, J. Phys. F **13**, 1547 (1983).
[42]G. Meyer, F. Hartmann-Boutron, Y. Gros, and I. A. Campbell, J. Magn. Magn. Mat. **46**, 254 (1985).
[43]G. Meyer, F. Hartmann-Boutron, and Y. Gros, J. Phys. (Paris) **47**, 1395 (1986).
[44]A. T. Ogielski, Phys. Rev. B **32**, 7384 (1985).
[45]I. A. Campbell, J. Phys. Lett. **46**, L1159 (1985); Phys. Rev. B **33**, 3587 (1986).
[46]I. A. Campbell, Hyperfine Int. **34**, 505 (1987).
[47]I. A. Campbell, J. M. Flesselles, R. Jullien, and R. Botet (unpublished).